Bioactive glass thin films synthesized by advanced pulsed laser techniques

N Mihailescu[1], George E Stan[2], C Ristoscu[1], M Sopronyi[1] and Ion N Mihailescu[1*]
[1] National Institute for Lasers, Plasma and Radiation Physics, 409 Atomistilor Street, Magurele, Ilfov, RO-77125, Romania;
[2] National Institute of Materials Physics, 405A Atomistilor Street, Magurele-Ilfov, RO- 077125, Romania

E-mail: ion.mihailescu@inflpr.ro

Abstract. Bioactive materials play an increasingly important role in the biomaterials industry, and are extensively used in a range of applications, including biodegradable metallic implants. We report on Bioactive Glasses (BG) films deposition by pulsed laser techniques onto biodegradable substrates. The BG coatings were obtained using a KrF* excimer laser source (λ= 248 nm, $\tau_{FWHM} \leq$ 25 ns). Their thickness has been determined by Profilometry measurements, whilst their morphology has been analysed by Scanning Electron Microscopy (SEM). The obtained coatings fairly preserved the targets composition and structure, as revealed by Energy Dispersive X-Ray Spectroscopy, Grazing Incidence X-Ray Diffraction, and Fourier Transform Infra-Red Spectroscopy analyses.

1. Introduction

Bone fractures caused by various unwanted accidents or different diseases heal at different times, depending on the type of fracture and patients age. Certain fractures in young kids can heal as quickly as 3 weeks, while it may take as long as 6 weeks for the same kind of fracture to heal in teenagers. And some fractures can take more than 10 weeks to mend [1]. It is expected that due to the increase of life expectancy and access to quality healthcare the number of people which will opt for implants will rise continuously, and thereby the demand for continuous innovation in this realm [2,3].

Nowadays, there is an increasing interest focused on coatings for biodegradable Magnesium-based metal implants. The idea of using a biodegradable metallic implant based on Mg is that can rapidly adapt to the body and eventually dissolve after the bone has healed [4,5]. But, besides good properties of Mg, like good biocompatibility, similar mechanical properties to natural bone, or lightweight metallic material, the main disadvantage is his rapidly corrosion rate in physiological environments. Consequently, they degrade faster than the time required for bone healing [6,7]. Consequently, this issue has stimulated numerous research teams around the world to test materials and combinations of materials as coatings on Mg-based metal implants to mitigate the fast corrosion rate [5,8]. The focus of this study concerns the development of biocompatible and biodegradable coatings by pulsed laser deposition (PLD) method of bioactive glasses (BG), on Mg-metallic implants with the intent of reducing and controlling the corrosion rate and increasing their biocompatibility. BG are made of various metal oxides combinations and are superior in bioactivity to calcium phosphates (e.g. hydroxyapatite, octacalcium phosphate) [9–11]. Moreover, after prolonged contact with body fluids *in vivo*, they change their composition transforming in an equivalent of the mineral bone [10,12].

It is widely accepted that laser-based technologies are among the main, most powerful tools for fabrication of micro- and nano-arrays of wide-range of different biomaterials with controlled thickness (with the precision of 1 Å), good adhesion to the substrate and specific surface properties [13]. Up to present time, PLD technique proved to be a versatile technique able to synthesize biomaterials thin films on temporary or biodegradable metallic substrates with improved corrosion properties and excellent biocompatibility [14–18]. The obtained results hint toward the development of alternative viable solutions for a new generation of biodegradable metallic implants with increased functionality.

2. Materials and Methods

2.1 Materials and experiment

Two bioactive glass formulations have been employed as PLD target in this study: 6P57 (wt.%: SiO_2-56.5%, Na_2O-11%, K_2O-3%, CaO-15%, MgO-8.5%, and P_2O_5-6%) and 6P61 (wt.%: SiO_2-61.1%, Na_2O-10.3%, K_2O-2.8%, CaO-12.6%, MgO-7.2%, and P_2O_5-6%). These two compositions are respectively slightly lower and higher than the threshold value of 60 wt.% SiO_2 which corresponds to a significant change in bioactivity and degradability of BG [9,10]. Two grams from each powder were pressed at 5 MPa in a 20 mm diameter mold (model Specac), and the resulting pellets were heat-treated in a furnace (model Carbolite CF1100), at 650°C/6 h, to reach compactness by eliminating air bubbles and water vapours.

PLD depositions were conducted inside a stainless steel deposition chamber using a KrF* excimer laser source, model *COMPexPro 205* (λ = 248 nm, $\tau_{FWHM} \leq 25$ ns), running at a repetition rate of 10 Hz. The laser beam was oriented with an inclination angle of 45° with respect to the target surface. The ablated material was collected either onto Mg disks (thickness=2 mm) or Si (100) wafers and were placed parallel to the targets (on-axis geometry), at a 40 mm separation distance.

During the experiments, the substrates were heated and maintained at a constant temperature of 450°C using a temperature controller (model PID-EXCEL). The depositions have been carried out at a residual pressure of 10^{-3} Pa and in oxygen atmosphere. The experimental conditions were identical for both deposition substrates. Prior to introduction inside the deposition chamber, in order to eliminate the micro-impurities, the substrates were successively cleaned into an ultrasonic bath in acetone, ethanol and deionised water for 20 min and then blown dry with high purity nitrogen. The laser fluence on target was set at ~2.9 J/cm^2. The targets were continuously rotated with 0.3 Hz and translated along two orthogonal axes to avoid the formation of deep craters in order to insure a uniform deposition. This also allowed exposing a "fresh" surface to the action of every laser pulse. For the growth of one film, 20000 consecutive laser pulses were applied.

2.2 Film thickness determination and morphological examination

The coating thickness was monitored and estimated by profilometry using a Stylus Profiler HP-2 from Ambios Technology. A continuous scan at a rate of 10 μms^{-1} and 1 mm working distance were used. For statistics, the measurements were performed on three identical samples. Morphological characterization was carried out by Scanning Electron Microscopy (SEM) using a FEI Inspect S electron microscope, operating at 20 kV acceleration voltage, in high vacuum, under secondary electron mode.

2.3 Compositional and structural investigation

Compositional analysis was performed by Energy Dispersive Spectroscopy (EDS), with a SiLi EDAX Inc. detector, operated at 20 kV.

The long-range order of the simple BG films was investigated by grazing incidence X-ray diffraction (GIXRD) using a Bruker D8 Advance diffractometer, in parallel beam setting, with Cu K_α (λ=1.15406 Å) incident radiation. The incidence angle was set to 2°, and the scattered intensity was scanned within the 2θ range (15–45)°, with a step size of 0.04°, and 25 s per step.

Fourier Transform Infra-Red (FTIR) spectroscopy was employed for analysing the short-range order and nature of functional groups present in the BG films. The measurements were performed with a Perkin Elmer Spectrum BX II spectrometer, in attenuated total reflection mode (ATR) using a Pike-MIRacle diamond head of 1.8 mm diameter. The spectra were collected in the fingerprint wave numbers range 1300–550 cm^{-1}, by recording 128 individual scans at a resolution of 4 cm^{-1}.

3. Results and Discussion

The profilometry measurements in the case 6P57 and 6P61 coatings deposited in oxygen atmosphere indicated average thickness values in the range of ~4 μm. The coatings deposited in vacuum show different thicknesses depending on the type of BG composition: for 6P57≈7 μm and 6P61≈4 μm (figure 1).

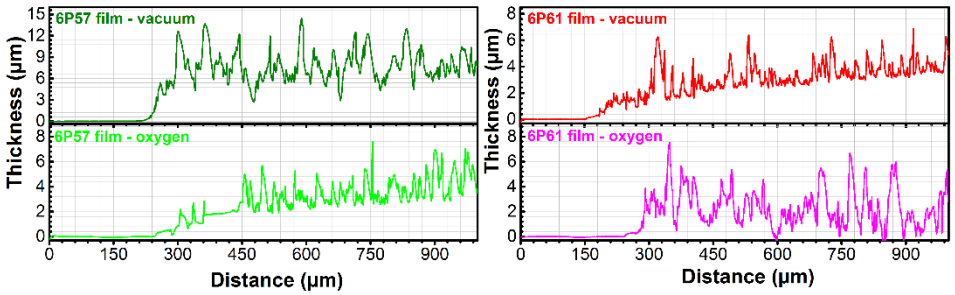

Figure 1. Thicknesses profiles of 6P57 and 6P61 coatings synthesized in oxygen or vacuum atmosphere by PLD method.

The surface morphology of 6P56 and 6P61 coatings deposited in oxygen atmosphere or in vacuum are illustrated in figure 2. It is noted that all coatings show uniform morphology, and consist of a homogenous matrix, consisting of particulates. At higher magnification, these morphological features appeared composed of isolated or merged spheroidal formations, with sizes in the micrometre range and an irregular distribution. Such particulates observed on the top of deposited coatings are characteristic to the PLD process [19]. Many studies demonstrated that these kinds of surfaces are beneficial for cells adhesion and growth [20–22].

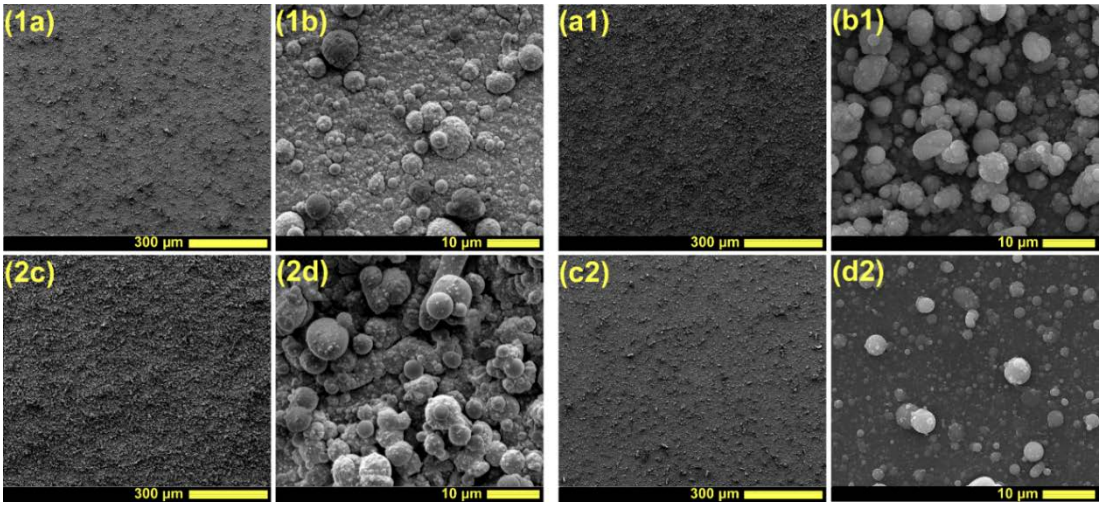

Figure 2. SEM images of 6P57 (1a,1b,2c,2d) and 6P61 (a1,b1,c2,d2) coatings deposited onto Si substrates in oxygen (1a,1b,a1,b1) and in vacuum (2c,2d,c2,d2). Panoramic (1a,2c,a1,c2 – magnification bar=300 μm) and detailed (1b,2d,b1,d2 – magnification bar=10 μm) views.

The EDS results for 6P57 and 6P61 coatings are presented in table 1. By comparing BG targets oxides concentration with the obtained coatings, after PLD transfer, it can be observed a good replication of the target materials' composition.

Table 1. Oxide concentration in wt.% of the BG coatings deposited by PLD onto Ti substrates (as estimated based on the quantitative EDS results). Network connectivity (NC) values.

	Oxide concentration (wt. %)						
Sample type	SiO_2	Na_2O	K_2O	CaO	MgO	P_2O_5	NC
6P57-vacuum	56.2±1.3	10.1±0.04	3.2±0.08	21.2±0.4	7.3±0.2	2.0±0.2	2.47
6P57-oxygen	58.2±2.0	10.8±0.06	2.8±0.07	17.1±0.5	7.4±0.2	3.7±0.3	2.73
6P61-vacuum	63.8±4.0	7.6±0.2	2.3±0.1	18.5±1.0	6.8±0.2	1.0±0.2	2.82
6P61-oxygen	61.1±1.8	9.8±0.03	2.5±0.1	15.3±0.5	7.5±0.2	3.8±0.1	2.89

The GIXRD analyses (figure 3) confirmed the amorphous status of the BG coatings regardless of the fabrication conditions.

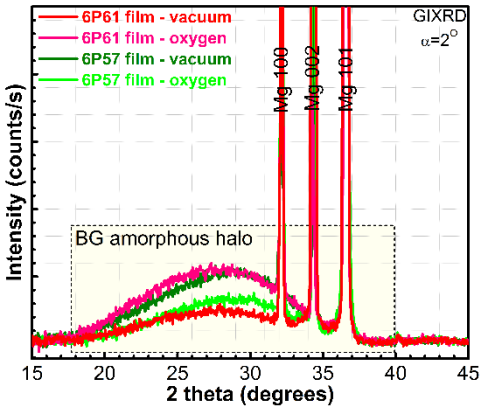

Figure 3. Comparative GIXRD patterns of BG coatings synthesized by PLD in vacuum and oxygen ambient.

The FTIR-ATR spectroscopic investigations evidenced the characteristic molecular vibrations of bonds and functional groups within the structure of either source raw glass powders, PLD targets (sintered at 650°C/6h in air), or BG coatings (figure 4a–c). The silica-based glasses consist of the tridimensional network formed of SiO_4 tetrahedral units (Q_{Si}^n; n=0–4, where n is the number of bridging oxygen atoms) interconnected at the corners by oxygen bridges. The glass network connectivity decreases with the increase of network modifiers (alkali and alkali-earth elements) concentration, because the charge compensation of the network modifiers occurs at the expense of oxygen bridges breaking. This way it is induced the formation of non-bridging oxygen structural units ($Si-NBO$: Q_{Si}^3; Q_{Si}^2; Q_{Si}^2; Q_{Si}^1; *and* Q_{Si}^0), whom concentration will govern the degradation speed of the glass in aqueous media, such as is the intercellular environment [9,10,23].

All analysed materials (raw powders, PLD targets, and BG coatings) elicited a broad IR band with two prominent shoulders centred at ~942 cm^{-1} (ascribed to the asymmetric stretching vibrations of the Si–NBO units) and at ~1001 cm^{-1} (associated with the asymmetric stretching vibrations of the Si–O–Si bonds). The lower intensity band, situated at ~776 cm^{-1}, is determined by the bending vibrations of

the Si–O bonds [24,25]. Due to the fairly low phosphorous concentration of the BG formulations used in this study, the characteristic vibrations of the phosphate functional groups cannot be easily evidenced, as they appear in the same spectral region [26,27] as the more intense absorption bands of the aforementioned silicate groups.

The comparison of the FTIR spectra of the raw powders and PLD targets (figure 4a) revealed that the sintering process applied at 650°C/6h does to induce compositional and structural modifications of the glass material. As expected, the Si–O–Si/Si–NBO ratio is higher in the case of the 6P61 glass, due to its elevated silica content, and consequently lower concentration of network modifiers.

In the case of both types of BG coatings synthesized under vacuum conditions a more reduced connectivity degree (determined by a higher amount of Si–NBO) has been signalled (figure. 4b,c). When oxygen is used as working gas during the PLD fabrication experiments an opposite tendency is noticed: both types of coatings experiencing an increase in intensity of the Si–O–Si band (figure 4b,c).

Thus, the preliminary studies have indicated so far that the control over the BG coatings' degree of network connectivity might be achieved by engineering the PLD working parameters.

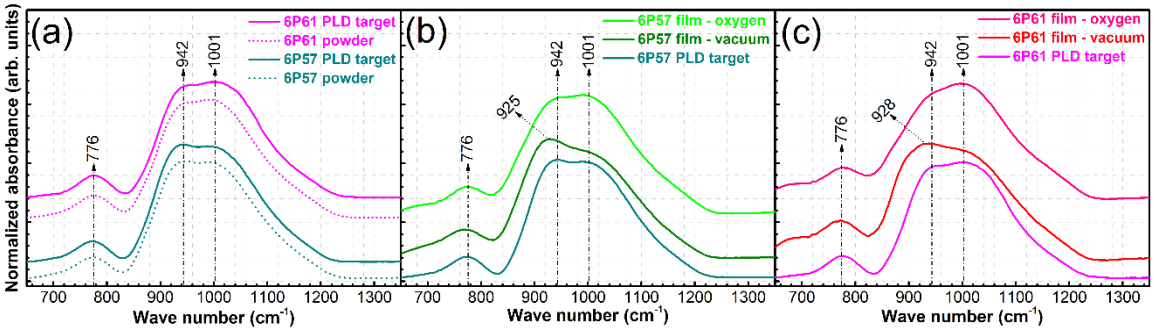

Figure 4. Comparative FTIR spectra of: (a) BG raw source powders and sintered PLD targets; (b) 6P57 PLD target and coatings; and (c) 6P61 PLD target and coatings.

4. Conclusions

BG coatings, with different concentration of silica were deposited on pure Mg and Si substrates, at a temperature of 450°C, by PLD technique in view of developing implants with controlled biodegradability. Preliminary morphological, compositional and structural assessments of the deposited coatings were conducted.

It was shown that the sintering process applied at 650°C/6h to PLD targets does not induced compositional and structural modifications of the glass material. The BG films displayed a rough morphology, suitable for osteointegration applications. The amorphous nature of all synthesized bioactive glass coatings was demonstrated. A better structure conservation was revealed in the case of films deposited under oxygen ambient. EDS has indicated the PLD method capacity to transfer near-congruently the complex composition of BGs on substrates.

We consider that the physico-chemical results recommend the further research of BG coatings fabricated by pulsed laser advanced techniques, as promising biomaterials fit to be integrated in biodegradable metallic implants.

Acknowledgements

N.M., C.R., M.S., and I.N.M. acknowledge with thanks the financial support of UEFISCDI under the contract TE140/2015. G.E.S. thanks the NIMP Core Programme PN 16 48-3/2016.

References

[1] http://kidshealth.org/en/parents/broken-arm.html;

[2] Floroian L, Ristoscu C, Mihailescu N, Negut I, Badea M, Ursutiu D, Chifiriuc M C, Urzica I, Dyia H M, Bleotu C and Mihailescu I N 2016 *Molecules* **21** 740
[3] http://www.marketsandmarkets.com/Market-Reports/orthopedic-device-280.html
[4] Adeosun S O, Lawal G I and Gbenebor O P 2014 *J. Miner. Mater. Charact. Eng.* **2** 88
[5] Bita A I, Stan G E, Niculescu M, Ciuca I, Vasile E and Antoniac I 2016 *J. Adhes. Sci. Technol.* **30** 1968
[6] Li Z, Gu X, Lou S and Zheng Y 2008 *Biomaterials* **29** 1329
[7] Hermawan H 2012 *Biodegradable Metals: From Concept to Applications* (Springer-Verlag Berlin Heidelberg)
[8] Hornberger H, Virtanen S and Boccaccini A R 2012 *Acta Biomater.* **8** 2442
[9] Hench L L 1991 *J. Am. Ceram. Soc.* **74** 1487
[10] Hench L L and Wilson J 1993 *Advanced Series in Bioceramics: Volume 1* (World Scientific Publishing Company, Singapore)
[11] Popa AC, Stan GE, Enculescu M, Tanase C, Tulyaganov DU and Ferreira JMF 2015 *J. Mech. Behav. Biomed. Mater.* **51** 313
[12] Floroian L, Popescu A, Serban N and Mihailescu I 2011 Polymer-bioglass composite coatings: A promising alternative for advanced biomedical implants *Metal, Ceramic and Polymeric Composites for Various Uses* ed. J Cuppoletti (Rijeka InTech) chapter 20 pp 393–420
[13] Pique A 2007 Deposition of polymers and biomaterials using the matrix-assisted pulsed laser evaporation (MAPLE) process *Pulsed Laser Deposition of Thin Films: Applications-Led Growth of Functional Materials* ed. R Eason (John Wiley & Sons, Hoboken NJ) chapter 3 pp 63–82
[14] Nelea V, Jelinek M and Mihailescu IN 2007 Biomaterials: New issues and breakthroughs for biomedical applications *Pulsed Laser Deposition of Thin Films: Applications-Led Growth of Functional Materials* ed. R. Eason (John Wiley & Sons, Hoboken NJ) chapter 18 pp 421–456
[15] Floroian L, Sima F, Florescu M, Badea M, Popescu A C, Serban N and Mihailescu I N 2010 *J. Electroanal. Chem.* **648** 111
[16] Mihailescu I N and Gyorgy E 1999 Pulsed Laser Deposition: An Overview *International Trends in Optics and Photonics* ed. T. Asakura (Springer-Verlag Berlin Heidelberg) chapter 13 pp 201-214
[17] Rau J V, Antoniac I, Fosca M, De Bonis A, Blajan A I, Cotrut C, Graziani V, Curcio M, Cricenti A, Niculescu M, Ortenz M and Teghil R 2016 *Mater. Sci. Eng. C* **64** 362
[18] Floroian L, Savu B, Stanciu G, Popescu A C, Sima F, Mihailescu I N, Mustata R, Sima L E, Petrescu S M, Tanaskovic D and Janackovic D J 2008 *Appl. Surf. Sci.* **255** 3056
[19] Eason R 2007 *Pulsed Laser Deposition of Thin Films: Applications-Led Growth of Functional Materials* (John Wiley & Sons, Hoboken NJ)
[20] Brunette D M, Tengvall P, Textor M and Thomsen P 2001 *Titanium in Medicine: Material Science, Surface Science, Engineering, Biological Responses and Medical Applications* (Springer, Berlin)
[21] Popa M, Hussien M D, Cirstea A, Grigore R, Lazar V, Bezirtzoglou E, Chifiriuc C, Sakizlian M, Stavropoulou E and Bertesteanu S 2015 *Curr. Top. Med. Chem.* **15** 1614
[22] Mihailescu N, Stan G E, Duta L, Chifiriuc M C, Bleotu C, Sopronyi M, Luculescu C, Oktar F N and Mihailescu I N 2016 *Mater. Sci. Eng. C* **59** 863
[23] O'Donnell M D 2012 Melt-Derived Bioactive Glass *Bio-Glasses: An Introduction* ed. JR Jones and A G Clare (John Wiley & Sons, Ltd, Chichester, UK) chapter 2 pp 13–27
[24] Popa A C, Marques V M F, Stan G E, Husanu M A, Galca A C, Ghica C, Tulyaganov D U, Lemos A F and Ferreira J M F 2014 *Thin Solid Films* **553** 166
[25] Popa A C, Stan G E, Besleaga C, Ion L, Maraloiu V A, Tulyaganov D U and Ferreira J M F 2016 *ACS Appl. Mater. Interfaces* **8** 4357

[26] Stuart B, Gimeno-Fabra M, Segal J, Ahmed I and Grant D M 2015 *ACS Appl. Mater. Interfaces* **7** 27362
[27] Stuart B W, Titman J J, Gimeno-Fabra M, Ahmed I and Grant D M 2016 *Mater. Des.* **111** 174